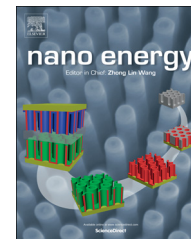Available online at www.sciencedirect.com

ScienceDirect

journal homepage: www.elsevier.com/locate/nanoenergy

nano energy

Self-powered metal surface anti-corrosion protection using energy harvested from rain drops and wind

Hua Rui Zhu[a,1], Wei Tang[a,1], Cai Zhen Gao[a], Yu Han[a], Tao Li[a], Xia Cao[a,*], Zhong Lin Wang[a,b,**]

[a]*Beijing Institute of Nanoenergy and Nanosystems, Chinese Academy of Sciences, Beijing 100083, China*
[b]*School of Material Science and Engineering, Georgia Institute of Technology, Atlanta, GA 30332-0245, United States*

Abstract

Corrosion of metal surfaces, especially ships and cultural relics, is one of the most concerns in asset protection, which costs billions of dollars worldwide each year. For the protection of metal surfaces, cathodic protection (CP) has been widely used as a primary technology. However, the application of the technology results in high energy cost and more serious environmental pollutions. In this work, a self-powered CP system for metal surface protection was designed by utilizing the energy harvested from natural rain drops and wind using a flexible triboelectric nanogenerator (TENG). The TENG power-supplying system can provide a practical energy source for sustainably driving the CP process without using an external power source. Stereoscopic microscopy, AC impedance measurements, polarization test and surface tension testing were used to verify the feasibility of self-powered CP process. Our results indicate that the flexible TENG can produce highly efficient CP system for almost all metallic structures. This work not only demonstrates a highly-simple-fabrication, great-performance and cost-effect approach to protect metal surfaces from corrosion, but also develops a new self-powered electrochemical technique for CP that can be widely used in metal cultural relics, ocean engineering, industry, transportation, and so on.
© 2014 Elsevier Ltd. All rights reserved.

Introduction

Corrosion of metal surfaces in areas such as battle ships and metal historic relics costs billions of dollars worldwide each year [1–4]. The corrosion mechanism of the metal surfaces is an electrochemical process that occurs in a thin electrolyte,

*Corresponding author.
**Corresponding author at: Beijing Institute of Nanoenergy and Nanosystems, Chinese Academy of Sciences, Beijing 100083, China
E-mail addresses: caoxia@binn.cas.cn (X. Cao),
zlwang@gatech.edu (Z.L. Wang).
[1]Hua Rui Zhu and Wei Tang contributed equally to this work.

and it is accelerated in rainy days. The most effective protection measures are surface treatments and coating techniques [5-7]. Among them, cathodic protection (CP) is widely used as a primary technology [8]. Generally, there are two typical CP systems: the first one is the sacrificial anode cathodic protection (SACP) system, in which the metal is electrically coupled to a sacrificial anode; the second is the impressed current cathodic protection (ICCP) system, in which a cathodic current is applied from an external power source that is connected between an 'inert' anode electrode and the metal to be protected. For the SACP system, more active metals are sacrificed to protect the specimen from corrosion, and what's more, the protected area is limited to the size of sacrificed metal [9]. For the ICCP system, external power sources are required to provide sufficient output, resulting in very high cost and environmental pollutions [10]. In recent years, other CP systems have been reported, such as photogenerated cathode protection, however, an ultraviolet light source is required in the system [11–14]. Since corrosion is a slow process, and anti-corrosion could also be a slow process, therefore, an ideal CP system should be a self-powered system that operates by harvesting available energy from environment (kinetic energy of rain drops and wind) without supplying an additional power source.

Recently, the triboelectric nanogenerator (TENG) has been invented as an effective approach to convert ambient mechanical energy into electricity [15-18], by using the coupling of triboelectrification and electrostatic induction [19]. Compared with traditional power sources, TENG has the advantages of simple fabrication, large electric output, excellent robustness, and low cost [20-26]. What's more, TENG can easily harvest many types of mechanical energy including human activities, waves lapping, wind blowing, raining and so on, which could be significantly high enough for protecting metal surfaces from corrosion [27,28].

In this paper, we designed a self-powered CP system for metal surface protection by utilizing the energy harvested from wind and rain drops using a flexible TENG. During the rainy season, metal surface can experience an accelerated corrosion. At this time, the self-powered CP system driven by TENG can protect the metal surface from corrosion. To the best of our knowledge, it is the first time that a self-powered CP system for metal surface protection is reported. Our research demonstrates that the flexible TENG can produce highly efficient CP system for almost all of metallic structures. Considering the extremely-low cost, non-polluting and unique applicability, the as-established self-powered CP system can also be widely used in ocean engineering and industrial equipment protection.

Results and discussion

In order to characterize the feasibility of the self-powered CP system, the electrical characteristics of the flexible TENG were investigated. The TENG is based on the contact electrification of polydimethylsiloxane (PDMS) and ITO (Figure 1a and b). Before fabrication of TENG, PDMS was pretreated to form inverted pyramid structures (Figure 1c). Figure 1d and e shows the output current and voltage of the TENG under stimulations at a frequency of 1 Hz. As we can

see, the output current is over 130 μA, and the voltage reaches about 500 V. CP experiments of metal surface were conducted with and without the CP of TENG. For the one powered with TENG, the cathode was the protected specimen that was immersed into the electrolyte and the anode was a carbon rod (Figure 1f). The TENG was rectified and then connected to the whole system with the external stimulation at a frequency of 1 Hz. Corrosion data are compared and discussed in the following sections. Furthermore, when raining, TENG can harvest the mechanical energy of wind and rain drops, and then convert them into electricity to provide the power for the CP. Since the TENG can be driven by human motions, wind and rain drops, it can power up multiple light-emitting diodes (LEDs) by harvesting the ambient mechanical energy. As shown in Figure 1g and h, the multiple LEDs were powered up (detail process see Videos S1-S3 in the Supporting information), which indicated the self-powered CP system is feasible.

Supplementary material related to this article can be found online at http://dx.doi.org/10.1016/j.nanoen.2014.11.041.

Generally speaking, rusts can intuitively reflect the corrosion degree of metal surface. Then, the rusted specimens with and without CP system were studied under microscopy to compare their micro-morphology after accelerated corrosion test. As shown in Figure 2, for the specimens protected with CP system, there are several gray distributing areas on the surface and the gray distributing areas increase with corrosion time elapsed. However, no apparent corrosion was observed on these samples. On the other hand, for the specimen without the CP driven by TENG, pitting were observed clearly in the three pictures, and more big pits were found on the sample that was corroded in simulated electrolyte for 72 h. The macro-morphology analysis of specimens also showed the same corrosion states (Figure S1, Supporting information). The micro and macro-morphology analysis demonstrate that the CP system can protect the specimens from corrosion effectively. Further, the specimens without the CP driven by TENG corroded deeply as the corrosion time increased, however the specimens with the CP system have not been corroded obviously.

In order to evaluate the corrosion degree and protectiveness of the corrosion products, AC impedance measurements were performed in this work. Nyquist diagrams of the specimens after accelerated corrosion with and without the CP driven by TENG are given in Figure 3a and b. It is evident that within the frequency range of the measurement, the diagrams of the specimens with and without the CP systems reveal different features qualitatively.

For the specimens with CP systems (Figure 3a), the impedance spectra show a typical Faraday control process, in which radius of arcs represents the charge transfer resistance (R_t) of the electrochemical reaction [29]. The smaller the radius of arcs is, the lower of the reaction resistance is, and the electrochemical reaction more easily happens on the metal surface. In the other words, that means little or no protective rust layer on the specimen surface. The radius of arcs induced by the specimen corroded for 24 h is the smallest, followed by that corroded for 48 h and 72 h. To interpret the impedance spectra, an adequate electrochemical model is needed. Based on the fitting procedure of impedance data, an appropriate equivalent circuit was selected for analysis of the corrosion process (inset of Figure 3a).
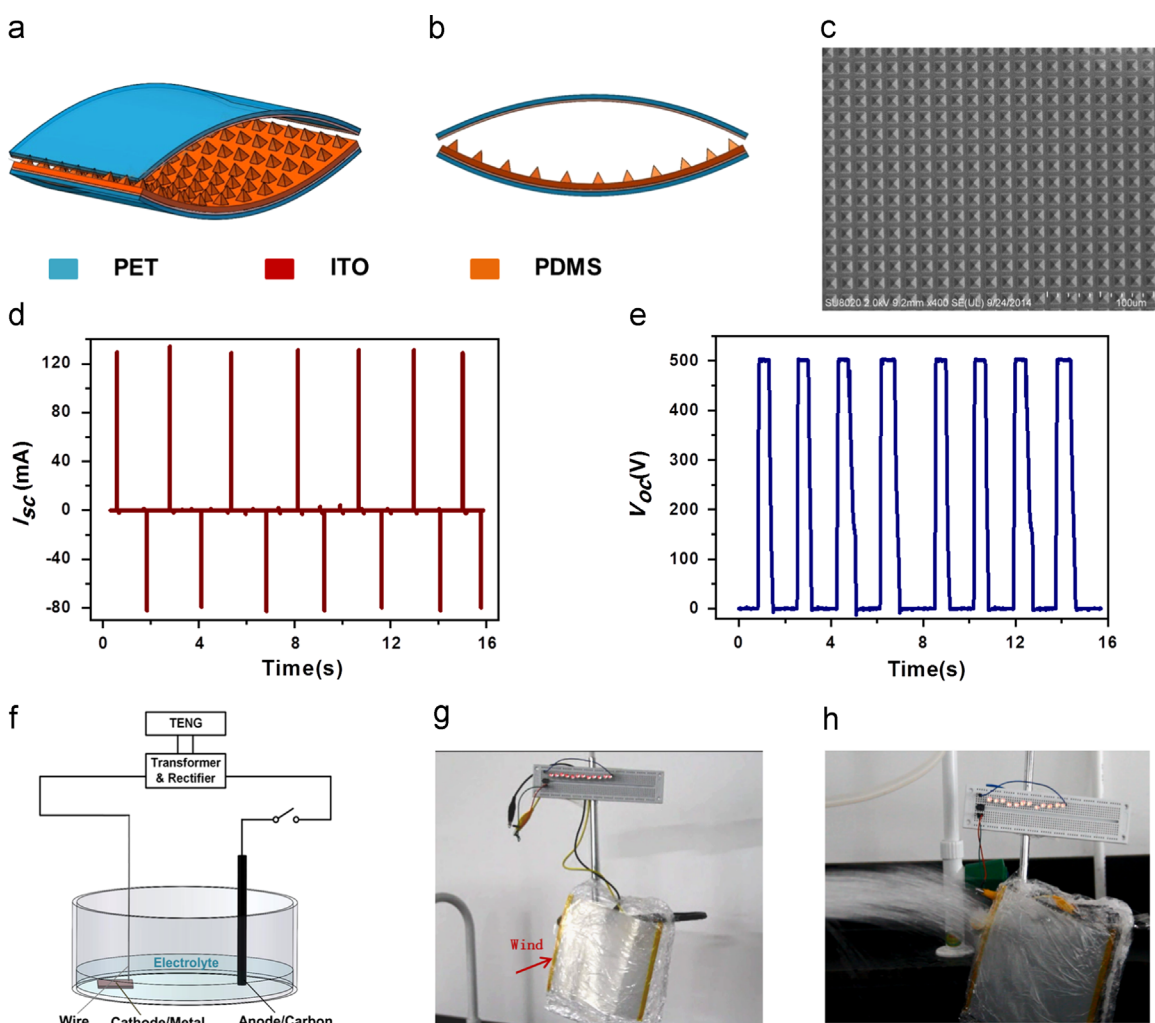
Figure 1 (a) Scheme of the designed TENG, (b) profile of the TENG; (c) SEM image of PDMS' pyramid structures; (d) Short circuit currents and (e) open circuit voltages of TENG at a frequency of 1 Hz. (f) Schematic diagram of the metal surface CP system driven by TENG. (g) Lighted LEDs as driven by wind blowing; and (h) lighted LEDs as driven by rain drops.

In the equivalent circuit of specimens in the measurement process, R_s and R_t were the solution resistance and charge transfer resistance, respectively. C_d was the double layer capacitance in parallel with R_t. In the present case, R_t was assumed to be equal to the polarization resistance R_p, which provided a reasonable estimate of the corrosion rate. The R_t was obtained from the curve fitting procedure, which was summarized in Table 1. For the specimen with CP driven by TENG, the value of R_t is small-that is, rust layer did not form on the metal surface. In other words, non-protective film formed on the specimens with the CP system.

For the specimens without the CP driven by TENG, the influence of the rust layer on specimens was investigated by AC impedance, too. In order to evaluate how protective the rust was, impedance measurement of rusted specimen after different corrosion time was carried out. The EIS data were shown in Figure 3b. It can be seen that all of the three impedance spectra corresponding to Nyquist diagrams exhibit a slightly distorted capacitive semicircle at high frequencies and a diffusion tail line in the low frequency region. The characteristics show that the electrochemical reaction was controlled both by Faraday process and diffusion process [29].

The depressed semicircle in high frequency range is attributed to the charge transfer resistance and the double layer capacitance. As we know, the Warburg impedance corresponds to the diffusion process. The phase angel of the diffusion tail deviates from 45°, which relates to a slow diffusion process on the corrosion layer. As shown inset of Figure 3b, the impedance spectra were fitted using the equivalent circuit model, too. R_{ct} represents the charge transfer resistance of the electrochemical reaction. C_f and R_f are the capacitance and resistance of solid electrolyte interface film, respectively. Q is associated with the capacitance of the double layer and passivation film (rusted layer). W represents the diffusion-controlled Warburg impedance. R_e corresponding to the ohmic resistance is relatively small and can be ignored. The fitting results of R_{ct} according to the equivalent circuit model are presented in Table 1. For the specimens without CP system, the values of R_{ct} are larger than the values with CP system and increase as the corrosion time extending. The higher the charge transfer resistance, the slower the electrochemical kinetic reaction, and the more protective the rusted layer. That is to say, protective film formed on the specimens without the CP system.
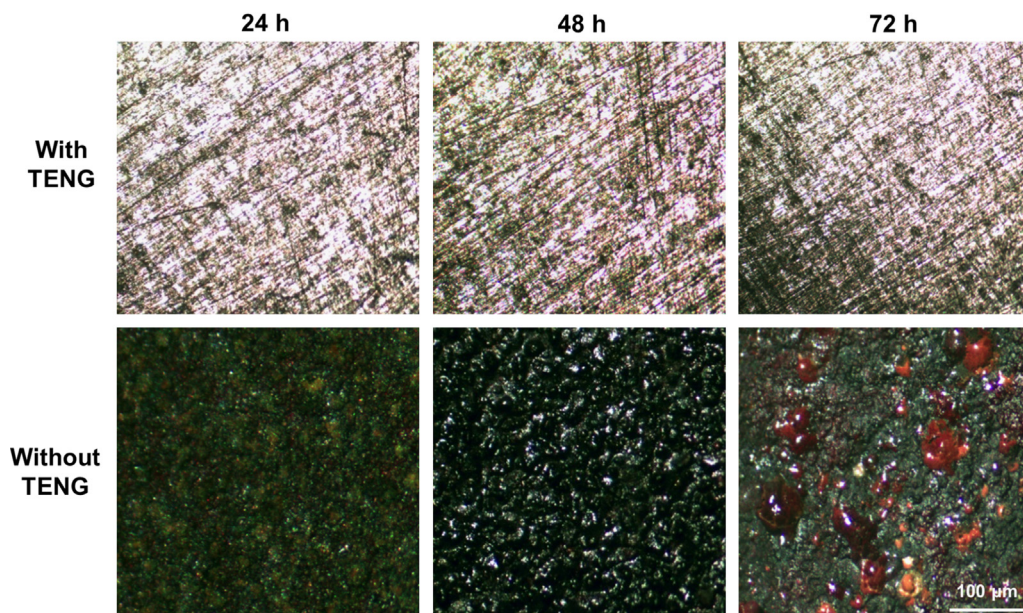
Figure 2 Micrographs of the rusted specimens after accelerated corrosion. The specimens were separated into two groups; one group (the tops) were under CP driven by TENG while the other ones (the bottoms) were not.
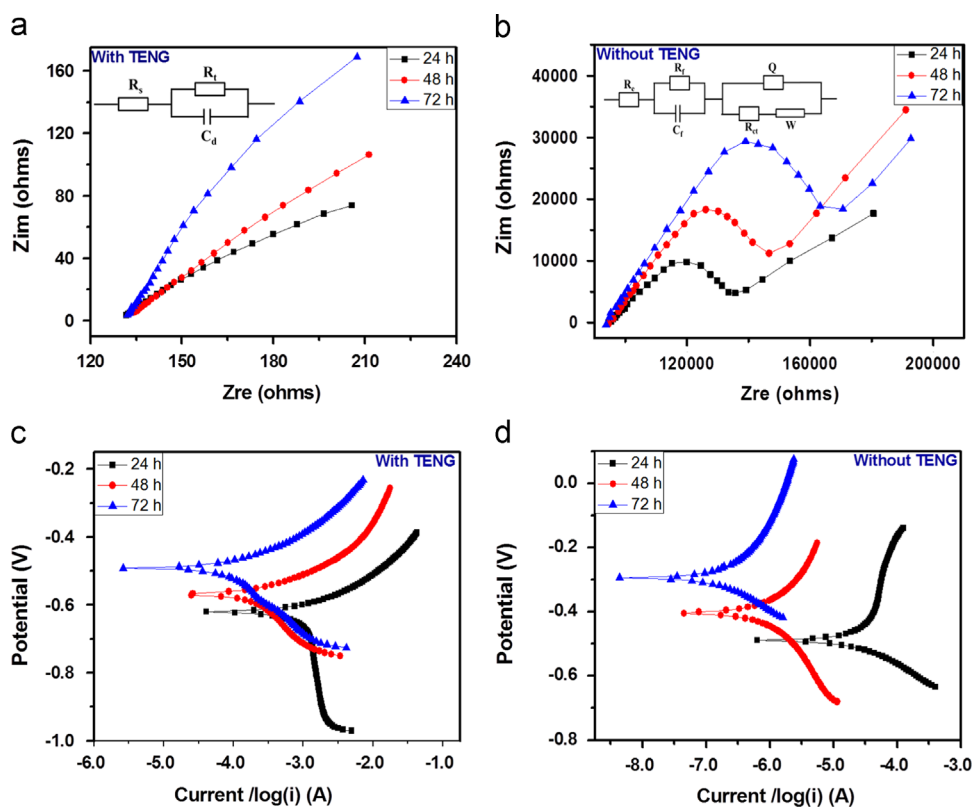

Figure 3 Nyquist plots of the specimens after accelerated corrosion with (a) and without (b) the CP systems, inset: equivalent circuit of specimens in measurement systems, respectively. Polarization curves of the specimens after accelerated corrosion with (c) and without (d) the CP driven by TENG.

At the same time, we measured the polarization plots of every specimen which experienced accelerated corrosion. From Figure 3c and d, we found that the polarization currents of specimens which were protected with TENG are higher than that without the CP system. However, the polarization currents all decrease with the corrosion time elapsed for two kinds of specimens. Interestingly enough, the polarization potential of the rust specimen reverses to the polarization current, that is the polarization potential of the specimen with the CP driven by TENG is lower than

Table 1 The charge transfer resistance of specimens with and without the CP driven by TENG.

	24 h	48 h	72 h
R_t with-TENG	0.21	0.45	0.73
R_{ct} without-TENG	16.34	46.23	78.52

that without the CP system and the polarization potentials all increase with the corrosion time elapsed. These data demonstrate the CP system can protect the specimen surfaces from corrosion and the rust layer on the specimen surface can protect them from further corrosion [30]. The results were consistent with AC impedance data.

The rust layer on the specimen has significant effects on the hydrophilic property of sample. To verify the corrosion degree of specimen surfaces further, the surface tension and adsorption rate were quantified and compared by measuring the respective contact angles. Photos and contact angles of macro-size droplets placed on the specimen surfaces were shown in Figure 4 and Table 2. From these data, we can judge easily that the adsorption rate on specimen surface without the CP system is faster than that with the CP and the adsorption rate increases with time elapsing for all samples. For the specimen with the CP system, the corrosion rate is very slow, so the specimen surface is hydrophobic. As the corrosion time elapsed, several rust dots generated on the specimen surface and the contact angels of water drops on the specimen decreased. For the specimens without the CP system, HSO_3^-, NO_3^- as substitute for oxygen to participate in the corrosion process, this can contribute to the anodic dissolution and cause the generation of $FeSO_4 \cdot 7H_2O$, $FeSO_4 \cdot 9H_2O$, $Fe(NO_3)_2 \cdot 6H_2O$ and γ-FeOOH [31]. As seen from Figure 2, the rust layer was rough and loose. That's why the contact angles of water drops on the specimen surface decreased. The faster the absorption rate of the specimens is, the deeper of the corrosion degree it has been in the accelerated corrosion process. The surface tension tests further confirm that the CP system driven by TENG is an effective way to protecting metal surface from corrosion.

In order to compare the corrosion degree of specimens with and without the CP systems quantitatively, corrosion data of the specimens were measured by weight loss tests. These data were only recorded when the specimens had already been uniformly treated. The weight-loss data of the samples placed in the simulated electrolyte with and without the CP driven by the TENG are shown in Figure 5. It is observed that the corrosion rate of samples without the CP system is about 10 times higher than the one when the power from TENG was applied at the same corrosion times. Furthermore, the corrosion data were fitted by using the well-know bilogarithmic equation approximately [32]:

$$C = At^B \tag{1}$$

where C is the weight loss (g), t is the periodic test time (h), A and B are the constants. A is equivalent to the weight loss when time is unity and B reflects the change in weight loss tests with time. The table in Figure 5 lists the regression coefficients of the corrosion data from the weight-loss test.

From Figure 5, we can observe that the corrosion rate of samples without the CP is higher during the corrosion process
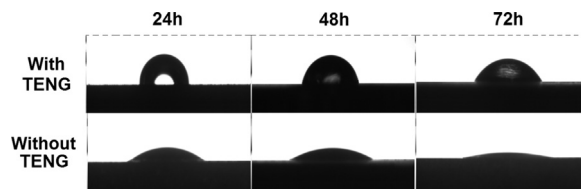
Figure 4 Pictures of micro-droplets on rusted specimen surfaces after accelerated corrosion. The specimens were separated into two groups, one group (the tops) were protected by CP system while the other ones were not.

Table 2 Contact angles of water drops on the liquid/specimen interfaces.

	With TENG			Without TENG		
t_r (h)	24	48	72	24	48	72
C.A. (°)	91.6	74.0	53.6	36.2	15.2	6.75

t_r: The corrosion times, C.A.: the average value of contact angles.

in the test and increase notably as time elapses. However, corrosion rates induced by the sample with the CP driven by TENG do not increase apparently as corrosion proceeds. It is well known that constant B is roughly equal to 0.5 of the corrosion which is controlled by an ideal diffusion process; if the value of B is smaller than 0.5, it means a decrease in diffusion coefficient and the rust layer becomes more protective. Thus the rust layer induced by the corrosion without the CP of TENG is more protective than that with TENG according to the value of B as showed in Figure 5. The results also demonstrate that the CP powered from TENG is feasible in the protection for metal surface.

Conclusions

In summary, we have developed the first self-powered CP system for metal surface protection driven by flexible TENG using the energy provided by wind and rain drop in the environment. Systematic investigations were carried out to compare the corrosion degree of metal surface with and without the CP system. Our results confirm that the metal surfaces with the CP driven by TENG show no apparent corrosion, while the others without the CP system corroded heavily in the same simulated environment. The work demonstrates a highly simple fabrication, strong performance and cost-effect approach to protecting metal surface from corrosion. The new technique of self-powered electrochemical CP system can be used in metal cultural relics, ocean engineering and transportation.

Experimental section

Preparation of specimen

The cast iron was used as the sample to simulate metal corrosion. The chemical composition of the specimens (wt%) was: C 0.02, Si 0.01, Mn 0.03, P 0.04, S 0.003, Fe 99.8. The specimens were sectioned into 30 mm × 30 mm × 3 mm and
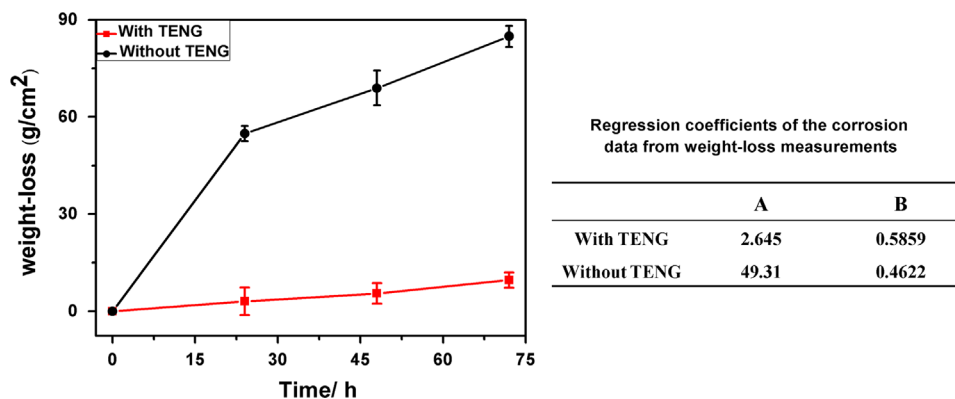
Figure 5 Weight-loss curves of testing specimens after accelerated corrosion and the regression coefficients of the corrosion data from weight-loss measurements.

were grounded with 600-grit paper. Then they were washed in acetone and methanol, quickly dried and kept in nitrogen atmosphere prior to the test.

Fabrication of the self-powered CP system

The basic structure of the CP system is composed of a TENG device and an electrochemical corrosion model system, as schematically illustrated in Figure 1. The TENG is based on the contact electrification of PDMS and ITO. The PDMS elastomer and cross-linker were mixed in a 10:1 ratio (w/w) and degassed for 20 min. Then the mixture was coated on to a silicon mold, which was previously patterned with inverted pyramid structures. After cured at 85 °C for 60 min in an oven, the PDMS film was peeled off from the silicon substrate, and then transferred on to an ITO-coated polyester (PET) film. Subsequently, another clean ITO-coated PET film was placed onto the prepared PDMS-ITO-PET film and sealed at the two ends. It is worth noting that the PDMS surface and the ITO electrode are placed face to face, leaving a small gap of 5 mm between the two contact surfaces by forming an arched structure. The effective size of the TENG cell is 15 cm × 15 cm, and the thickness under pressed is about 1 mm. The output voltage and current were measured by the Keithley 6514 System Electrometer and SR570 low noise current amplifier from Stanford Research Systems [33]. In the corrosion model system, the cathode was the protected specimen that was just immersed into the electrolyte and the anode is carbon rod.

Simulated accelerated corrosion test

The accelerated test was conducted in an exposure box. 0.1 M $NaHSO_3$+0.1 M $NaNO_3$ electrolyte was used to simulate the polluted environment and the specimens were just immersed into the 0.1 M $NaHSO_3$+0.1 M $NaNO_3$ solution to simulate the thin liquid layer on the metal surface in raining days. The corrosion rate was calculated by weight loss test at periods of 24 h, 48 h, and 72 h with and without the CP powered by TENG. After a period of time, the specimens were rinsed with distilled water, degreased and scrubbed with cotton balls to remove the corrosion products. The remainder of the corrosion products was immersed in 50% H_2SO_4 at ambient temperature [34]. In the end, specimens

were dried in an oven at 80 °C for an hour and weighed to 0.1 mg.

Characterization of surface appearance

The study on corrosion product of the rusted specimen was performed using a SZ660TP stereoscopic microscopy for surface analysis. Stereoscopic microscopy images were recorded by using 50 (objective) × 20(ocular) magnifier.

Electrochemical tests

A PARSTAT 4000 system manufactured by Princeton Applied Research was used to undertake electrochemical impedance and polarization curve measurements. A Princeton flat cell three-electrode system was selected in which the reference electrode was Ag/AgCl, and the counter electrode was a platinum foil. The exposed area of specimens was 10 mm × 10 mm.

Interface tension test

Interface tension test was accomplished by OCA40 Micro Data physics Instruments (GmbH Germany) and OCA20 contact-angel system. The corrosion degree of the specimen was determined by measuring the respective contact angles of drops on the archaeological cast iron. To make the macro-size solution droplet, 5 μl distilled water was put on to the metal surface using a suitable micro-syringe. Macro-size droplets with diameters of 0.5-5 mm were placed onto the specimen surface. Then, the edge and the region around it were observed carefully by a laser microscope. Wave length of the laser was 632.8 nm for this experiment.

Appendix A.   Supporting information

Supplementary data associated with this article can be found in the online version at http://dx.doi.org/10.1016/j.nanoen.2014.11.041.

References

[1] L. Gianni, G.E. Gigante, M. Cavallini, A. Adriaens, Materials 7 (2014) 3353.
[2] M. Quaranta, E. Catelli, S. Prati, G. Sciutto, R. Mazzeo, J. Cult. Herit. 15 (2014) 283.
[3] G. Poggi, N. Toccafondi, L.N. Melita, J.C. Knowles, L. Bozec, R. Giorgi, P. Baglioni, Appl. Phys. A 114 (2014) 685.
[4] J. Muller, B. Laïk, I. Guillot, Corros. Sci. 77 (2013) 46-51.
[5] R. Bhaskaran, N. Palaniswamy, N.S. Rengaswamy, M. Jayachandran, Anti-corros. Methods Mater. 52 (2005) 29.
[6] R. Singh, N.B. Dahotre, J. Mater. Sci.: Mater. Med. 18 (2007) 725.
[7] C.Q. Ye, R.G. Hu, S.G. Dong, X.J. Zhang, R.Q. Hou, R.G. Du, C.J. Lin, J.S. Pan, J. Electroanal. Chem. 688 (2013) 275.
[8] M.M.S. Cheung, C. Cao, Constr. Build. Mater. 45 (2013) 199.
[9] J.G. Kim, J.H. Joo, S.J. Koo, J. Mater. Sci. Lett. 19 (2000) 477.
[10] J. Xu, W. Yao, Build. Mater. 23 (2009) 2220.
[11] J.N. Yuan, S. Tsujikawa, J. Electrochem. Soc. 142 (1995) 3444.
[12] C.F. Chen, C.H. Shen, C.L. Lin, Thin Solid Films 377 (2000) 326.
[13] Y. Ohko, S. Saitoh, T. Tatsuma, A. Fujishima, J. Electrochem. Soc. 148 (2001) 24.
[14] H. Yun, C.J. Lin, J. Li, J.R. Wang, H.B. Chen, Appl. Surf. Sci. 255 (2008) 2113.
[15] F.R. Fan, Z.Q. Tian, Z.L. Wang, Nano Energy 1 (2012) 328.
[16] G. Zhu, J. Chen, Y. Liu, P. Bai, Y.S. Zhou, Q.S. Jing, C.F. Pan, Z.L. Wang, Nano Lett. 13 (2013) 2282.
[17] Y.S. Zhou, Y. Liu, G. Zhu, Z.H. Lin, C.F. Pan, Q.S. Jing, Z.L. Wang, Nano Lett. 13 (2013) 2771.
[18] J.W. Zhong, Q. Zhong, F.R. Fan, Y. Zhang, S.H. Wang, B. Hua, Z.L. Wang, J. Zhou, Nano Energy 2 (2013) 491.
[19] Y. Higashiyama, K. Asano, Part. Sci. Technol. 16 (1998) 77.
[20] S. Lee, Y. Lee, D. Kim, Y. Yang, L. Lin, Z.-H. Lin, W. Hwang, Z.L. Wang, Nano Energy 2 (2013) 1113.
[21] S. Wang, L. Lin, Y. Xie, Q. Jing, S. Niu, Z.L. Wang, Nano Lett. 13 (2013) 2226.
[22] J. Chen, G. Zhu, W. Yang, Q. Jing, P. Bai, Y. Yang, T.-C. Hou, Z.L. Wang, Adv. Mater. 25 (2013) 6094.
[23] G. Zhu, C.F. Pan, W.X. Guo, C.Y. Chen, Y.S. Zhou, R.M. Yu, Z.L. Wang, Nano Lett. 12 (2012) 4960.
[24] L. Lin, Y.F. Hua, C. Xua, Y. Zhang, R. Zhang, X.N. Wen, Z.L. Wang, Nano Energy 2 (2013) 75.
[25] T.-C. Hou, Y. Yang, H.L. Zhang, J. Chen, L.-J. Chen, Z.L. Wang, Nano Energy 2 (2013) 856.
[26] Z.L. Wang, G. Zhu, Y. Yang, S.H. Wang, C.F. Pan, Mater. Today 15 (2012) 532.
[27] W.X. Guo, X.Y. Li, M.X. Chen, L. Xu, L. Dong, X. Cao, W. Tang, J. Zhu, Ch-J. Lin, C.F. Pan, Z.L. Wang, Adv. Funct. Mater. 24 (2014) 6691.
[28] Z. Wang, L. Cheng, Y.B. Zheng, Y. Qin, Z.L. Wang, Nano Energy 10 (2014) 37.
[29] D.M. Drazic, J.P. Popic, J. Serb. Chem. Soc. 70 (2005) 489.
[30] F. Mansfeld, Corros. Sci. 47 (2005) 3178.
[31] C.S. Castro, M.C. Guerreiro, L-C-A Oliveira, M. Goncalves, Quim. Nova 32 (2009) 1561.
[32] L. Veleva, P. Castro, G. Hernandez-Duque, M. Schorr, Corros. Rev. 16 (1998) 235.
[33] F.R. Fan, J.J. Luo, W. Tang, C.Y. Li, C.P. Zhang, Z.Q. Tian, Z.L. Wang, J. Mater. Chem. A 2 (2014) 13219.
[34] W.G. Whitman, R.P. Russell, C.M. Welling, J.D. Cochrane, Ind. Eng. Chem. 15 (1923) 672.

Hua-rui Zhu received her Ph.D. degree from Institute of High Energy Physics, Chinese Academy of Sciences (CAS) in 2014. She now is the research assistant in Beijing Institute of Nanoenergy and Nanosystems, CAS. Her research interests include the energy materials, nanobiosensors, piezoelectric sensors and self-powered electrochemistry.

Wei Tang received his Ph.D. degree from Peking University in 2013. He visited CMI of EPFL to participate in a Swiss-China joint Project in 2012. His research interests are micro/nano-devices, principle investigation of triboelectric nanogenerators, power transformation & management, and self-powered wireless sensing network.

Cai-zhen Gao is currently pursuing master's degree in Chemistry under the supervision of Prof. Wang and Prof. Cao at Beijing University of Aeronautics and Astronautics and Beijing Institute of Nanoenergy and Nanosystems, Chinese Academy of Sciences. Her dissertation is focused on the nanobiosensors and piezoelectric sensors.

Yu Han is currently pursuing her master's degree in Applied Chemistry under the supervision of Prof. Wang and Prof. Cao at Beijing University of Aeronautics and Astronautics and Beijing Institute of Nanoenergy and Nanosystems, Chinese Academy of Sciences. Her dissertation is focused on application of bimetallic nanomaterials to electrocatalysis and biosensors.

Tao Li received his B.C. in Material Chemistry (2011) and M.S. in Material Physic and Chemistry (2014) from Lanzhou University. Now he is a Ph.D. student at the Beijing Institute of Nanoenergy and nanosystem, Chinese Academic Science. His current research mainly focuses on energy harvesting and fabrication of nanodevices.

Xia Cao received her Ph.D. degree from department of Materials Physics and Chemistry in Beijing University of Chemical Technology. She is currently a professor at Beijing Institute of Nanoenergy and Nanosystems, Chinese Academy of Sciences. Her main research interests focus on the energy materials, nanoelectroanalytical chemistry, nano-biosensors and piezoelectric sensors.

Zhong-lin (Z.L) Wang received his Ph.D. from Arizona State University in physics. He now is the Hightower Chair in Materials Science and Engineering, Regents' Professor, Engineering Distinguished Professor and Director, Center for Nanostructure Characterization, at Georgia Tech. Dr. Wang has made original and innovative contributions to the synthesis, discovery, characterization and understanding of fundamental physical properties of oxide nanobelts and nano-wires, as well as applications of nanowires in energy sciences, electronics, optoelectronics and biological science. His discovery and breakthroughs in developing nanogenerators established the principle and technological roadmap for harvesting mechanical energy from the environment and biological systems for powering a personal electronics. His research on self-powered nanosystems has inspired the worldwide effort in academia and industry for studying energy for micro-nano-systems, which is now a distinct disciplinary in energy research and future sensor networks. He coined and pioneered the field of piezotronics and piezo-phototronics by introducing piezoelectric potential gated charge transport process in fabricating new electronic and optoelectronic devices. Details can be found at: www.nanoscience.gatech.edu.